ESCUELA DE CONSTRUCCIÓN CIVIL
FACULTAD DE INGENIERÍA

Revista de la Construcción
Journal of Construction

Research Article

Mechanical performance of ETC RC beam with U-framed AFRP laminates under a static load condition

P. Loganathan[1*], R. Mohanraj[2], S. Senthilkumar[3], K. Yuvaraj[4]

1 Department of Civil Engineering, Excel Engineering College, Komarapalayam, Namakkal, Tamilnadu (India); Email: iplogu@gmail.com
2 Department of Civil Engineering, Excel Engineering College, Komarapalayam, Namakkal, Tamilnadu (India); Email: rsrirammohan@gmail.com
3 Department of Civil Engineering, KSR College of Engineering, Thiruchengode, Namakkal, Tamilnadu (India); Email: senthilkumarcivil@ksrce.ac.in
4 Department of Civil Engineering, KSR College of Technology, Thiruchengode, Namakkal, Tamilnadu (India); Email: yuva02raj@gmail.com
*Correspondence: email: iplogu@gmail.com

Received: 05.01.2022; **Accepted:** 06.12.2022; **Published:** 29.12.2022

Citation: Loganathan, P., Mohanraj, R., Senthilkumar, S., and Yuvaraj, K. (2022). Mechanical performance of ETC RC beam with U-framed AFRP laminates under a static load condition. Revista de la Construcción. Journal of Construction, 21(3), 678-691. https://doi.org/10.7764/RDLC.21.3.678.

Abstract: In the presented paper, an attempt has been made to first find the permeability of the Euphorbia tortilis cactus (ETC) concrete by the water permeability method and infiltration method. After that, the flexural strength of the ETC RC beam wrapped with AFRP kelvar 149 is carried out by a 2-point load test. This research aimed to develop a more durable, flexural, and sustainable beam under static load. Based on the state-of-the-art information available in the literature, 3-layer Kelvar 149 AFRP is considered as a laminate to solve the deflections of the ETC beam. In this project, RCC beams were strengthened by ETC and aramid FRP sheets. Novel results are obtained by different layers and patterns of Aramid FRP sheets. Based on the investigation 3-layers Kelvar 149 perform well than a normal concrete beam. As no result based on hydraulic conductivity and drying shrinkage of a beam with AFRP laminates are available in the literature, the obtained results are validated with the finite element method (ABAQUS) under static load conditions.

Keywords: Aramid fiber reinforced polymer, kelvar 149, rehabilitation, hydraulic conductivity test, euphorbia tortilis cactus.

1. Introduction

Cement composite is the most extensively utilized construction material in the construction division. Throughout their projected lifetime, concrete structures are supposed to withstand physical, chemical, and weathering impacts while still keeping the desired technical qualities (Hanehara & Yamada, 1999). Often, degradation and failure occur before the predicted lifetime due to micro cracks development and fluids' subsequent entry into these structures. The setting and curing characteristics of the concrete, cement paste, or mortar at the time of production affect durability performance. Though concrete strength and durability is a potential problem, which is governed by several factors such as lower values of compressive strength, a high chance of clogging, and less resistance to corrosion in severe environments.

Lime was the primary binder utilized in ancient times. Concrete and mortar made of lime have poor durability and strength. Utilizing organic material increased a structure's durability (Bezerra, 2016). The majority of these materials were inexpensive and easily accessible locally. They are referred to as natural additives. Chandra (Chandra, Eklund, & Villarreal, 1998) has discussed the background of natural polymers over time. However, some efforts to increase the moisture resistance of concrete structures have utilized costlier and perhaps regionally inaccessible materials. In addition, latex from the rubber plant was employed as a water-proofing paint on brickwork in Africa and South America (Cárdenas, Goycoolea, & Rinaudo, 2008). Boiling banana plant stems and leaves was a common method for producing paint in other cultures. According to Ernesto et al., employing stabilizers produced by cactus plants considerably increased the moisture resistance of adobe walls (Izaguirre, Lanas, & Álvarez, 2011).

The durability of concrete is a potential problem (Jonkers, Mors, Sierra-Beltran, & Wiktor, 2016), which is governed by several factors such as lower values of compressive strength, a high chance of clogging (Jensen & Hansen, 2001), and less abrasion resistance under dynamic loading. The use of FRP composites and ETC to strengthen Reinforced Cement Concrete (RCC) beams (Martínez-Barrera, Gencel, Reis, & del Coz Díaz, 2017) is becoming increasingly common. For many reasons, Aramid FRP is more convenient than steel. The usage of advanced fiber reinforced polymer/plastics (FRP) composites to reinforce reinforced concrete beams has grown in popularity in recent years.

It is because the structure: (i) may require alteration due to aging (Lasheras-Zubiate, Navarro-Blasco, Fernández, & Álvarez, 2012), (ii) Corrosion in steel induced by exposure to a hostile environment may cause it to deteriorate (Kyomugasho, Christiaens, Shpigelman, van Loey, & Hendrickx, 2015), (iii) may require strengthening to withstand accident loads such as earthquakes, etc (Jumadurdiyev, Hulusi Ozkul, Saglam, & Parlak, 2005). Flexural failure and shear failure are the two important failure modes in any flexural member. The former is a ductile failure at first, but brittle is later. A ductile failure distributes stress and alerts occupants, whereas brittle collapse occurs suddenly and is consequently disastrous. To strengthen the flexural members against this brittle failure, different strengthening techniques/materials are commonly adopted.

FRP is one of the strengthening materials recommended instead of steel for several reasons. Compared to steel, this FRP material has a higher ultimate strength and lower density, is easier to no interim support until it reaches its full strength. This material may be easily shaped into complex shapes and cut to the desired length on the job site. Fibres are normally classified as GFRP, CFRP(Kizilkanat, 2016), and AFRP. From a structural standpoint, FRP is primarily used in two areas. The first is the use of FRP sheets/plates to reinforce structural components using externally applied FRP. The focus on potential enhancements to toughness and durability offered by synthetic macro fibers helps to develop new applications of AFRP (Al-Jabri, Hisada, Al-Oraimi, & Al-Saidy, 2009). Steel is easier to install, requires no interim support until it reaches its full strength, and has a higher ultimate strength but a lower density than Aramid FRP.

Some of the most widespread plants in the world right now are cactus plants. Cactus plants are ubiquitous. It is a xerophytic plant with a height range of 5-7 meters (Peschard, Govin, Grosseau, Guilhot, & Guyonnet, 2004). Modified leaves or flowers are the cactus edible portions. Crowns are the name given to the leaves. It is crown grown with a width of 3m and its diameter may vary up to 1m. Succulents and cactus plants are frequently confused with one another. Given that both of these plants are xerophytes, which means they have certain characteristics that make them ideal for survival (Peschard et al., 2006), it makes sense. Water tends to be stored in the tissues of cacti (Zaharuddin, Noordin, & Kadivar, 2014). Cacti rely on the days' worth of water that is stored in their plant to survive. Cactus plants naturally can get water into the plant as soon as possible because they typically grow in dry environments (Togerö, 2006). They struggle, nevertheless, to get rid of extra water. As a result, if you keep giving your cactus plant more water than it can handle, it will start to experience problems. Euphorbia tortilis cactus extract is popular in the west and southern parts of Tamilnadu, among the many various types of plant-derived extracts that have been utilized as concrete additives. The plant is abundantly available in warm areas and may be easily picked and processed to create the organic addition, making it an ideal organic additive (Poinot, Govin, & Grosseau, 2013).

Additionally, it is anticipated that the calcium carbonate precipitation (Wei, Guo, & Zheng, 2016) in the concrete will improve the structure's strength. It's crucial to understand that fibers clog concrete pores not only because of their smaller size because of their smaller size and carbonate when exposed to air and moisture through cracks install, and requires it (Pourchez

et al., 2006). This calcium carbonate that has precipitated aids in filling the crack, lowering the likelihood of more cracks spreading.

2. Materials and methods

2.1. Cement

The most significant component of concrete is cement. One of the most significant factors to consider when choosing cement is its capacity to improve the microstructure of concrete. (Wu, Que, Cui, & Lambert, 2019)Natural additives were used in the ETC concrete, unlike the normal concrete. (Wee, Suryavanshi, & Tin, 1999)For ETC concrete to be achieved, the appropriate grade and quality of cement must be chosen. Fineness, alkali content, compressive strength at various ages, the heat of hydration, dicalcium Silicate (C_2S) content, tricalcium Silicate (C_3S) content, tricalcium aluminate (C_3A) content, and compatibility with admixtures (Hazarika et al., 2018) are some of the important factors that play a role in the selection of the type of cement. The type of cement chosen is determined by SCC's overall requirements, such as strength, and durability. Due to differences in compound composition and fineness, different brands of cement have been shown to exhibit variable strength development characteristics and rheological behavior. Ordinary Portland cement, grade 53, conforming to IS: 12269 – 2013 and IS:4031-1988, was utilized in this study. The cement is tested according to the coal processes, which are listed in Table 1.

2.*2 Fine aggregate*

As a fine aggregate, natural river sand from the locally available Karur River with a fraction passing through 4.75mm and held on a 600m sieve was used in this study.(Wei et al., 2016) The sand is cleansed and screened on-site to remove harmful elements before being tested according to the technique outlined in IS: 2386-1963 (Reaffirmed 2011). Table 1 shows the selected mechanical parameters. The test results confirmed that the sand comes under Zone III.

2.*3 Coarse aggregate*

Concrete's coarse aggregate is the most durable and least permeable component.(Shen, Wang, Cheng, Zhang, & Jiang, 2016) Crushed granite coarse aggregate provides greater interlocking and hence helps to obtain higher strength than rounded gravel aggregate in terms of aggregate shape(Yuvaraj & Ramesh, 2021). ETC Concrete can be made with coarse aggregate that meets the standards of IS: 383-1970. For this study, angular coarse aggregates with a maximum size of 20 mm were chosen, taking into account all of the above factors. Table 1 shows the results of testing coarse aggregates according to the techniques specified in IS: 2386-1963 (Reaffirmed 2011) and IS 383-1970 (Reaffirmed 2011).

2.4 Steel

The steel of grade Fe 415 (HYSD) of 6 mm, 8 mm, and 12 mm diameters were used (Shanmugasundaram, Mohanraj, Senthilkumar, & Padmapoorani, 2022) 12 mm diameter bars are utilized as tension reinforcement, and 8mm diameter bars were employed as hanger bars 6mm diameter bars were utilized for shear stirrups.

Table 1. Physical properties of materials.

Physical property	Cement	FA	CA
Specific gravity	3.15	2.66	2.76
Fineness modulus	2.32	3.71	7.42
Water absorption	-	0.6%	0.5%
Consistency	30.5%	-	-
Initial setting time	34 min.	-	-
Final setting time	10 hours	-	-

2.5 Aramid FRP sheet

Producing the Aramid fibers known as Kevlar, a registered brand, has special and advantageous qualities. Kevlar, a trademark of DuPont, is the name by which aramid fibers are commonly referred as. When Kevlar was first created in the 1960s, its chemical name was poly-para-phenylene terephthalate. Kevlar offers peculiar characteristics including exceptional impact resistance and low density. Table 2 includes information on the three different AFRP (Yahyaei-Moayyed & Taheri, 2011; Zhang et al., 2018) sheet patterns that were employed in this study. Kelvar 29 is reinforced with knitted mesh, Kelvar 49 is reinforced with chicken mesh, and kelvar 149 (Benmokrane, Zhang, & Chennouf, 2000; Toutanji & Deng, 2002) is reinforced with honeycomb. Figures 1, 2, and 3 depict the Kelvar 29, 49, and 149 forms, respectively.

Figure 1. Kelvar 29.

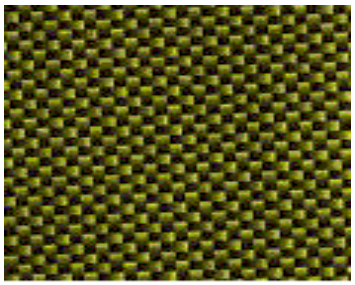

Figure 2. Kelvar 49.

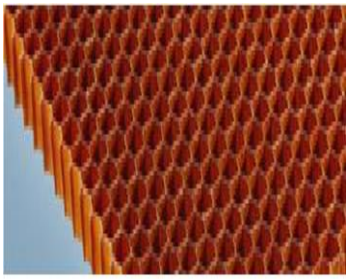

Figure 3. Kelvar 149.

Table 2. Properties of different AFRP sheets.

AFRP patterns	Density	Tensile strength	Modulus
Kelvar149	1.47 (g/cm3)	3650 MPa	174 GPa

3. Experimental results and analysis

3.1 Compressive tests on concrete cube

As per IS 10262-2000, Concrete mix proportion for M20 grade was designed. This code gives the design procedure using the properties of the material. The mix proportion of 1:1.63:2.96 (Cement: FA: CA) is obtained based on the mix design method. The water-cement ratio for this design is 0.41. The Compressive test results as shown in table 3.

Table 3. Compressive tests on concrete cube.

Test Specimen	Grade of concrete cube	Compressive strength at 28 days in N/mm^2
1	Reference concrete	22.5
2	9% ETC with M20 concrete	28.4

3.2 Hydraulic conductivity

3.2.1 Permeability

Using a falling head permeability test, the rate of water permeability through each specimen of concrete is determined. Permeability (k) is tested for cylindrical samples, as shown in Figure 4(a) and the test is conducted in accordance with IS: 3085 – 1965 code of practice. After being cured, the specimens are tested for 90 days (Nayak, 2021). The findings indicated that adding fine aggregate to the mixture significantly reduced the amount of water permeability. Because of the reduction in voids brought about by the addition of fines, the strength significantly increased. This further reduced the rate of water permeability. The rate of permeability was significantly influenced by porosity. The coefficient of permeability dropped along with the reduction in aggregate size. This is primarily due to the mix's decreased porosity. The use of ETC in concrete had little impact on permeability (Kilic & Gokce Gok, 2021). As a result, at all points of investigation, the mixes' porosity condition determines the rate of permeability. The water permeability value of the concrete can be calculated by equation 1.

$$k = (QL)/(Ah\Delta t), \qquad (1)$$

where, Q is the volume of discharge (m^3); L – is the specimen length (0.1 m); A – is the cross-section area of the cylinder (m^2); h – is the water head (m), and Δt – is the time interval (s).

3.2.2 Infiltration

It consists of two cylindrical rings, (Krishnaraja, Anandakumar, Jegan, Mukesh, & Kumar, 2019) one of diameter 300 mm (inner cylinder) and the other 600 mm (outer cylinder) placed over the slab specimen of size 1000 mm and depth 100 mm as shown in Figure 4(b). Initially, water is poured into the cylinder (Susilorini et al., 2014) and then the rapidity of infiltration of the water is noted using the scale attached with respect to the time and depth of infiltration into the slab specimen using Eq. 2. The values of the infiltration rate are given in Table 4.

$$I = (4V)/(3.14\, D_i^2\, \Delta t), \qquad (2)$$

where, V is the volume of water added in time Δt (m^3); D_i – the diameter of the inner cylinder (300 mm), and Δt – the time interval (s).

Table 4. Hydraulic conductivity test result.

Concrete mix	Permeability (k)		Infiltration (I)*	
	(cm/s (in./h))	(COV %)	(cm/s (in./h))	(COV %)
Nominal	1.31	23.1	0.30	2.3
M20 ETC	1.12	10.0	0.32	14.6
M20 ETC with AFRP	1.01	8.6	0.33	15.3

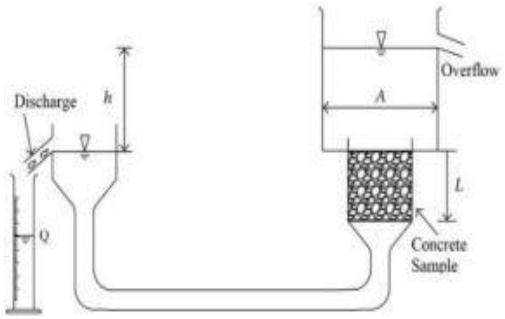

Figure 4 (a). Constant head permeameter.

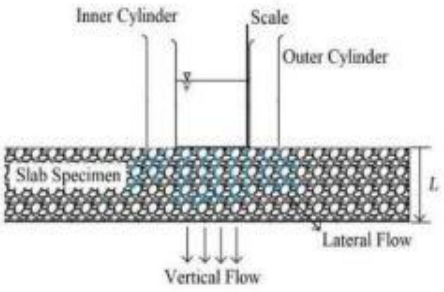

Figure 4 (b). Double ring infiltrometer.
Figure 4. Test setup for measuring permeability (k) and infiltration rate (I).

3.3 Drying shrinkage test on concrete

For measuring drying shrinkage, prismatic specimens with dimensions of 285 mm x 25 mm x 25 mm are employed. The test is conducted in accordance with the ASTM C596-09e1 code of practice (Sarfarazi, Ghazvinian, Schubert, Nejati, & Hadei, 2016). The starting lengths of the specimens are measured using a digital comparator with an accuracy of 0.001mm prior to transferring the demolded shrinkage specimens to the environmental chamber (40 percent relative humidity) after one day (Kong, Qi, Gu, Lawan, & Qu, 2018). The specimen is removed from the autoclave apparatus after a month, and any length loss is measured and reported. Measurements of drying shrinkage and autoclave apparatus are shown in Figure 5.

Figure 5. Deformation measurement.

3.4 Tests on beams

3.4.1 Experimental work

The experimental task entails casting M20 reinforced concrete (RC) beams with cross-sectional dimensions of 150 mm x 200 mm x 1000 mm.(Shanmugasundaram et al., 2022) At 160 mm c/c, we reinforced the base with 2-12 mm and the top with 2-8 mm Ø and 6 mm Ø vertical stirrups. Single Layer AFRP, Double Layers AFRP, and Triple Layers AFRP are three alternative patterns and layer combinations used to strengthen beams utilizing AFRP sheets. Totally, ten numbers of reinforced concrete beams have been cast and kept in water for curing for 28 days.

3.4.2 Setup for experimentation

All specimens are put through their paces in the loading frame, and the deflection is measured with an (LVDT) machine.

All of the samples are subjected to the same testing procedures. (Wang & Wu, 2010)After the 28-day cure time has concluded. Beams have three layers and three patterns, as well as conventional beams. The load arrangements for evaluating all sets of beams comprise two-point loading as illustrated in Figures 6(a) and 6(b).

3.4.3 Beam specification

The length of the Beam is 1000mm, the Span of the beam is 800mm, the width of the beam is 150mm, and the depth of the beam is 200mm.

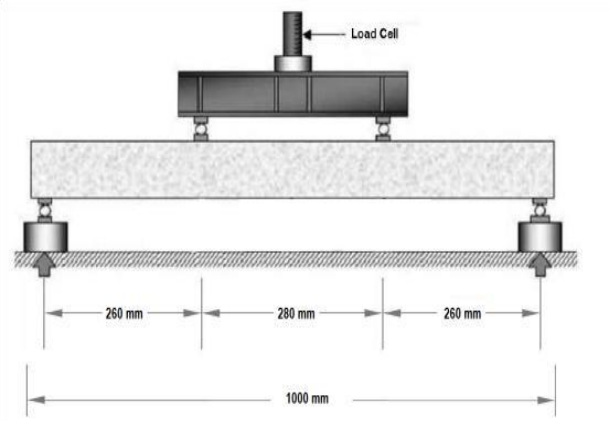

Figure 6 (a). Experimental setup for testing of beam.

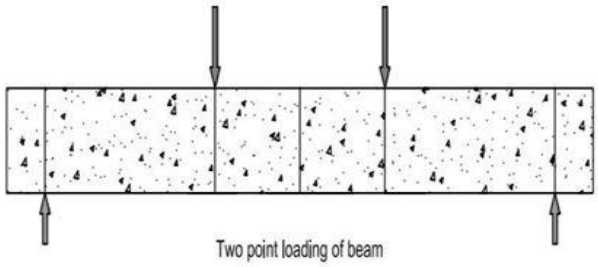

Figure 6 (b). Loading points over the beam.

3.4.4 Beam results

The performance of the specimen underuse of load was noticed. It was discovered that, with growing load, the cracks began to show up and constantly increment (Loganathan, Gracy, & Sharmila, 2022). Few cracks pass through the beam. The crack pattern has also been noticed. The values of load and deflection for the various volumes of reference concrete were listed in figure 7. It is seen that the bend followed a straight pattern until the first break load (Saafi & Toutanji, 1998). On the additional increase of load, numerous cracks were engendered and became complement as a definitive load was drawn nearer. The outcomes gotten show improved primary conduct, like those of FRP. If the number of layers' increases, the deflection against load decreases.

The values of load and deflection for the various volumes of ETC and Kelvar 149 were plotted in Figure 7. It is perceived that the bend followed a straight pattern until the first break load. On the additional increase of load, numerous cracks were engendered and became complement as a definitive load was drawn nearer.

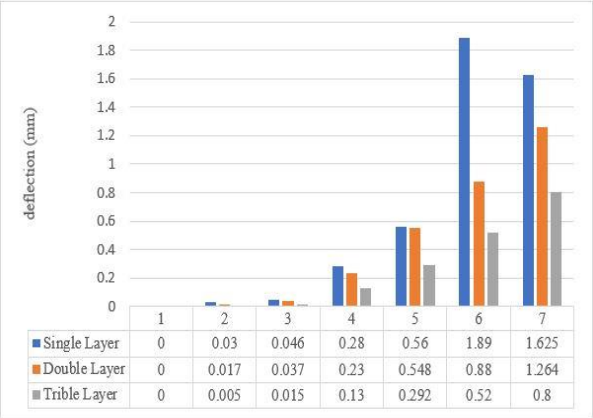

	1	2	3	4	5	6	7
Single Layer	0	0.03	0.046	0.28	0.56	1.89	1.625
Double Layer	0	0.017	0.037	0.23	0.548	0.88	1.264
Trible Layer	0	0.005	0.015	0.13	0.292	0.52	0.8

Figure 7. Deflection comparison of Kelvar 149 with various layers.

3.5 Analytical validation

The finite element method (FEM), a numerical analysis, can be used to find a rough solution to a variety of engineering problems. The finite element approach is now the most efficient technique for the numerical resolution of many engineering problems. In addition to stress analysis of solids, applications include the resolution of neutron physics, heat transfer problems, and acoustical phenomena.

Commercially available finite element analysis software for FEA goes by the name of ABAQUS. In addition to steady-state and transient problems, other problems include mode frequency and buckling analyses, electromagnetic and acoustic problems, various field and coupled-field applications, static and dynamic structural analysis (both linear and nonlinear), steady-state and transient problems, and more. The curriculum includes a Graphical User Interface (GUI) to aid new users in learning the topic. Users have access to a variety of tools, including toolbars, pull-down menus, dialogue boxes, multiple windows, and online documentation. Any geometry can be digitally represented using the collection of ABAQUS elements. ABAQUS supports a wide range of linear and nonlinear simulation applications. Multiple component problems can be modelled by matching the geometry of each piece with the appropriate material models and developing component interactions. During the nonlinear analysis, ABAQUS automatically selects the proper load increments and convergence tolerances and continuously modifies them to deliver an accurate result. Figure 8. Depict the reinforcement cage model, figure 9 Shows the assembling of RC beam in ABAQUS, figure 10 shows modelling of the RC beam, figure 11 depicts the strengthened beam with AFRP U trap, and figure 12 depicts the deformed shape of the beam with internal reinforcement, figure 13 Shows cracking of concrete and yielding of Steel, the corrosion of experimental and numerical results shown in figure 14.

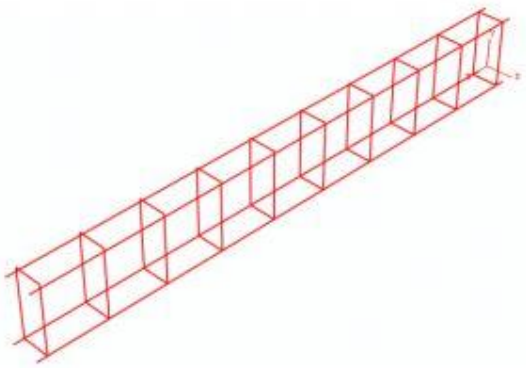

Figure 8. Reinforcement cage modeled in ABAQUS.

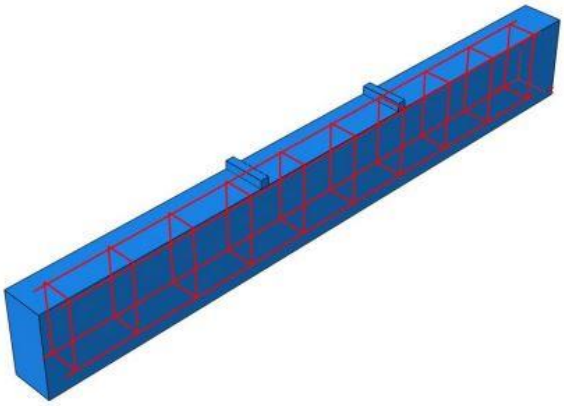

Figure 9. Assembling of the RC beam.

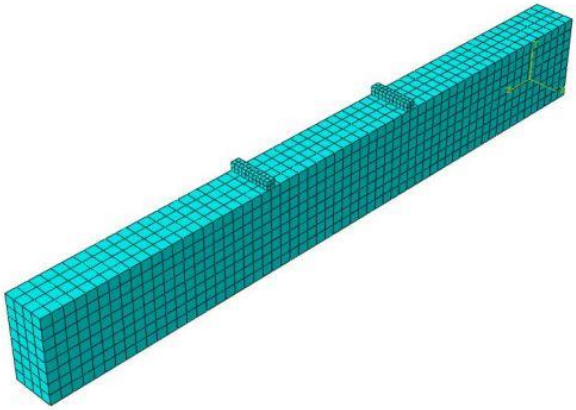

Figure 10. Meshing of RC beam model.

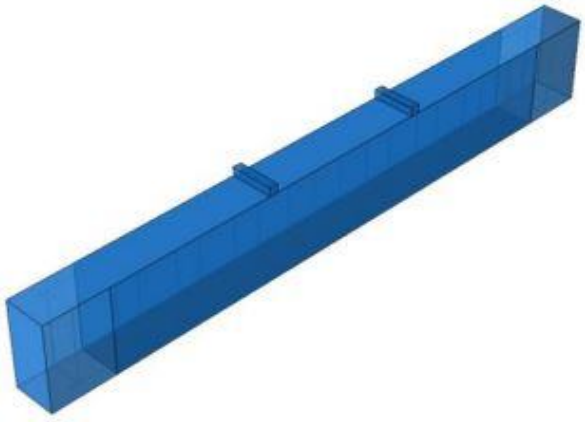

Figure 11. Strengthened beam with AFRP U wrap.

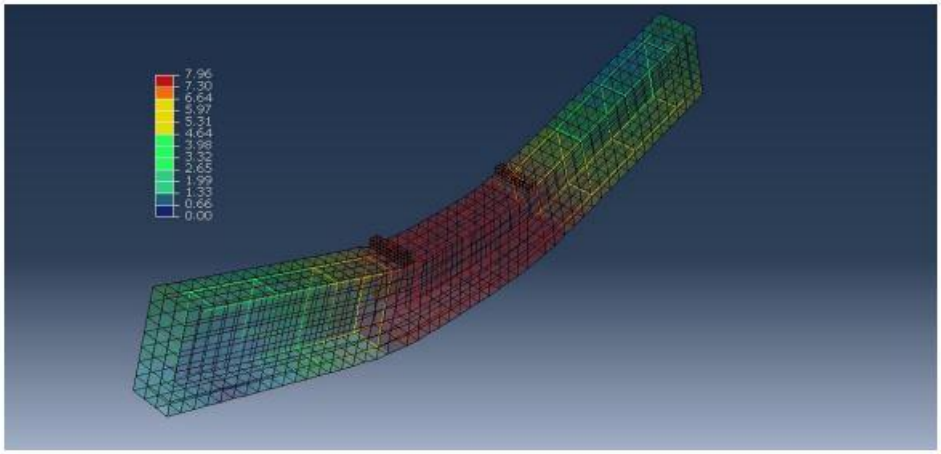

Figure 12. Deformed shape of the beam with internal reinforcement – control flexure.

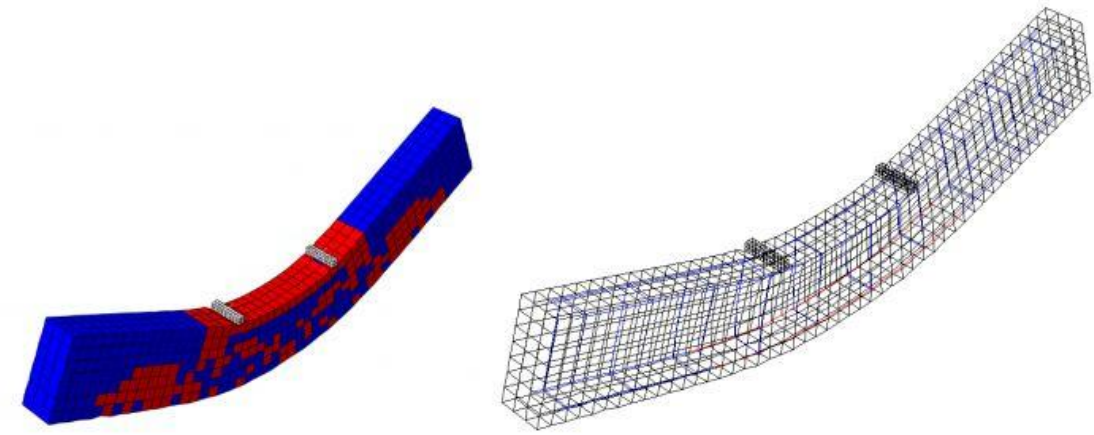

Figure 13. Cracking of concrete and yielding of steel.

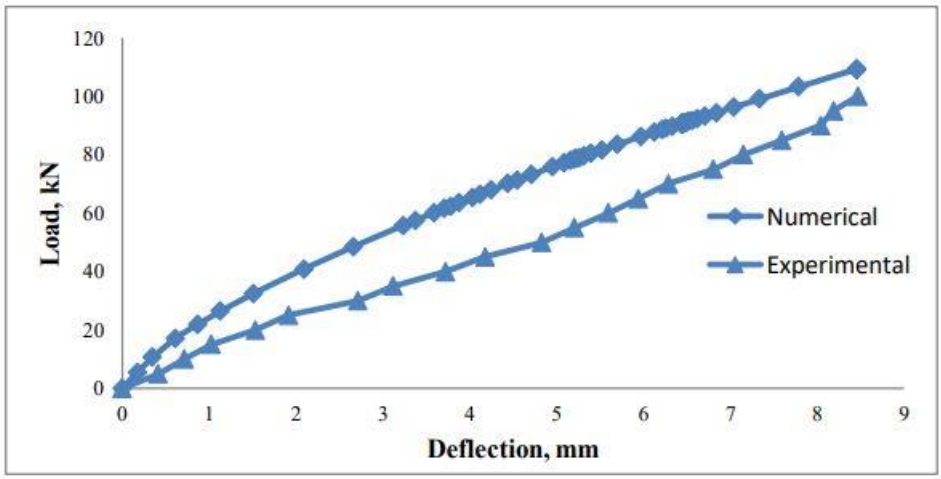

Figure 14. Load – deflection (strengthened beam shear deficient with AFRP – sides).

Selective RC members have undergone nonlinear finite element analysis (FE) both with and without strengthening. For simulation, the nonlinear properties of steel and concrete are taken into account. ABAQUS, a finite element program used for all purposes, has been used for FE modelling and analysis. To depict the nonlinear behavior of concrete, the widely used concrete damage model. By implementing the proper restriction conditions, including steel and concrete, the integrity of all the components, has been guaranteed. The responses, such as peak load and deformations, from the static nonlinear analysis, are compared with the relevant experimental findings. The FE analysis results closely match the corresponding experimental value, demonstrating the strength and dependability of the constructed FE models.

4. Conclusions and comments

1. The outcomes gotten show an increase in strength while increasing the layers. The deflection against load is less at three-layer kelvar 149. Physical properties of the materials, Hydraulic conductivity test, drying shrinkage, compressive strength of concrete cube, and tests on beams were determined and the results obtained are presented.
2. The research provided in the manuscript has led to the following broad conclusions. An innovative way for enhancing the flexural and shear behaviour as well as the serviceability of damaged concrete beams is the use of an AFRP strip bonding system. As a result of the characteristics mismatch between concrete and the repair material, it is free from the shortcomings of the already used approaches.
3. The uniformity in flow percentage of a freshly mixed concrete mix was negatively related to the aggregate size and fiber length. The test samples' permeability and penetration rate are decreased by the addition of macro synthetic fibers. This has been found to be especially important for high doses of long fibers. Comparing the infiltration rate to the permeability values of the equivalent mixture, the infiltration rate was nearly five times lower.
4. ETC-contained concrete mixes outperformed traditional concrete in terms of compressive strength. For 9% ETC concrete, the maximum improvement in compressive strength of 22.08% is achieved. Concrete mixtures incorporating ETC had lower water absorption values than conventional concrete, resulting in better pore plugging than conventional concrete.
5. Three RC beams that were not damaged have been strengthened utilizing hybrid laminates. Three specimens in each pattern—three at the bottom alone, three along the side faces, and three more in a U pattern were wrapped on the beams of one with ETC and one with AFRP laminates that were each 3mm thick. The typical maximum load and maximum deflection for bottom-strengthened RC beams are about 100 kN and 9.25 mm, respectively. It is obvious that the beams strength has increased by about 30% when compared to the control beams. At an average maximum load of 115kN and an average maximum deflection of 10.86mm, the hybrid-wrapped specimens in the U pattern failed. The strength has increased and is 40kN greater than the control beams in this wrapping pattern. The average maximum load and average maximum deflection when utilizing AFRP to strengthen the beams along the sides are 95kN and 8.75mm, respectively. When the beams are reinforced along the sidewalls alone, the strength increases by around 20%.
6. Similar to regular RC beams, the most common failure mode of retrofitted RC beams is a flexural failure, which involves the yielding of steel followed by the crushing of concrete. Performance-wise, the triple layer outperforms both the double layer and the single layer. Additionally, it was shown that the impact of fiber length was not as significant as the impact of aggregate size. As a result, it can be said with confidence that AFRP is one of the best ways to retrofit damaged ETC RC flexural parts because it has several advantages over steel plates and FRP laminates. It may be inferred from the whole analysis that retrofitting RC beams improves ductility in addition to strength.
7. The effect of a sudden release technique should be further examined. Additional research is needed for Aramid fiber-reinforced polymer members with different types of concrete (i.e., lightweight concrete, high-performance concrete, etc.).

Author contributions: Conceptualization: P. Loganathan, and R. Mohanraj; Methodology, R. Mohanraj, and S. Senthilkumar; Investigation: P. Loganathan, R. Mohanraj, S. Senthilkumar and K. Yuvaraj; Writing - original draft: P. Loganathan, and R. Mohanraj; Writing - review & editing: P. Loganathan, R. Mohanraj, S. Senthilkumar and K. Yuvaraj; Funding acquisition:

P. Loganathan, R. Mohanraj, and K. Yuvaraj; Resources: P. Loganathan, and S. Senthilkumar; Supervision: S. Senthilkumar. The final draught of the manuscript has been read and approved by all contributors.

Funding: No funding was received from any funding agency.

Acknowledgments: This research is supported by Excel Engineering College, KSR College of Engineering, and KSR College of Technology. The author would like to thank M/s. Modern Builders Pvt. Ltd. For providing the strands for this research. The author also would like to thank a number of individuals at the College campus for their contribution to this research.

Conflicts of interest: No conflicts of interest are disclosed by the authors.

References

Al-Jabri, K. S., Hisada, M., Al-Oraimi, S. K., & Al-Saidy, A. H. (2009). Copper slag as sand replacement for high performance concrete. *Cement and Concrete Composites*, 31(7), 483–488. Retrieved from https://doi.org/10.1016/j.cemconcomp.2009.04.007

Benmokrane, B., Zhang, B., & Chennouf, A. (2000). Tensile properties and pullout behaviour of AFRP and CFRP rods for grouted anchor applications. *Construction and Building Materials*, 14(3), 157–170. Retrieved from https://doi.org/10.1016/S0950-0618(00)00017-9

Bezerra, U. T. (2016). Biopolymers with superplasticizer properties for concrete. In *Biopolymers and Biotech Admixtures for Eco-Efficient Construction Materials* (pp. 195–220). Elsevier. Retrieved from https://doi.org/10.1016/B978-0-08-100214-8.00010-5

Cárdenas, A., Goycoolea, F. M., & Rinaudo, M. (2008). On the gelling behaviour of 'nopal' (Opuntia ficus indica) low methoxyl pectin. *Carbohydrate Polymers*, 73(2), 212–222. Retrieved from https://doi.org/10.1016/j.carbpol.2007.11.017

Chandra, S., Eklund, L., & Villarreal, R. R. (1998). Use of Cactus in Mortars and Concrete. *Cement and Concrete Research*, 28(1), 41–51. Retrieved from https://doi.org/10.1016/S0008-8846(97)00254-8

Hanehara, S., & Yamada, K. (1999). Interaction between cement and chemical admixture from the point of cement hydration, absorption behaviour of admixture, and paste rheology. *Cement and Concrete Research*, 29(8), 1159–1165. Retrieved from https://doi.org/10.1016/S0008-8846(99)00004-6

Hazarika, A., Hazarika, I., Gogoi, M., Bora, S. S., Borah, R. R., Goutam, P. J., & Saikia, N. (2018). Use of a plant based polymeric material as a low cost chemical admixture in cement mortar and concrete preparations. *Journal of Building Engineering*, 15, 194–202. Retrieved from https://doi.org/10.1016/j.jobe.2017.11.017

Izaguirre, A., Lanas, J., & Álvarez, J. I. (2011). Efecto de un polímero natural biodegradable en las propiedades de morteros de cal en estado endurecido. *Materiales de Construcción*, 61(302), 257–274. Retrieved from https://doi.org/10.3989/mc.2010.56009

Jensen, O. M., & Hansen, P. F. (2001). Water-entrained cement-based materials. *Cement and Concrete Research*, 31(4), 647–654. Retrieved from https://doi.org/10.1016/S0008-8846(01)00463-X

Jonkers, H. M., Mors, R. M., Sierra-Beltran, M. G., & Wiktor, V. (2016). Biotech solutions for concrete repair with enhanced durability. In *Biopolymers and Biotech Admixtures for Eco-Efficient Construction Materials* (pp. 253–271). Elsevier. Retrieved from https://doi.org/10.1016/B978-0-08-100214-8.00012-9

Jumadurdiyev, A., Hulusi Ozkul, M., Saglam, A. R., & Parlak, N. (2005). The utilization of beet molasses as a retarding and water-reducing admixture for concrete. *Cement and Concrete Research*, 35(5), 874–882. Retrieved from https://doi.org/10.1016/j.cemconres.2004.04.036

Kilic, I., & Gokce Gok, S. (2021). Strength and durability of roller compacted concrete with different types and addition rates of polypropylene fibers. *Revista de La Construcción*, 20(2), 205–214. Retrieved from https://doi.org/10.7764/RDLC.20.2.205

Kizilkanat, A. B. (2016). Experimental Evaluation of Mechanical Properties and Fracture Behavior of Carbon Fiber Reinforced High Strength Concrete. *Periodica Polytechnica Civil Engineering*, 60(2), 289–296. Retrieved from https://doi.org/10.3311/PPci.8509

Kong, X., Qi, X., Gu, Y., Lawan, I. A., & Qu, Y. (2018). Numerical evaluation of blast resistance of RC slab strengthened with AFRP. *Construction and Building Materials*, 178, 244–253. Retrieved from https://doi.org/10.1016/j.conbuildmat.2018.05.081

Krishnaraja, A. R., Anandakumar, S., Jegan, M., Mukesh, T. S., & Kumar, K. S. (2019). Study on impact of fiber hybridization in material properties of engineered cementitious composites. *Matéria (Rio de Janeiro)*, 24(2). Retrieved from https://doi.org/10.1590/s1517-707620190002.0662

Kyomugasho, C., Christiaens, S., Shpigelman, A., van Loey, A. M., & Hendrickx, M. E. (2015). FT-IR spectroscopy, a reliable method for routine analysis of the degree of methylesterification of pectin in different fruit- and vegetable-based matrices. *Food Chemistry*, 176, 82–90. Retrieved from https://doi.org/10.1016/j.foodchem.2014.12.033

Lasheras-Zubiate, M., Navarro-Blasco, I., Fernández, J. M., & Álvarez, J. I. (2012). Effect of the addition of chitosan ethers on the fresh state properties of cement mortars. *Cement and Concrete Composites*, 34(8), 964–973. Retrieved from https://doi.org/10.1016/j.cemconcomp.2012.04.010

Loganathan, P., Gracy, A. F. D., & Sharmila, S. M. R. (2022). An experimental investigation on corrosion impediment in R.C. slabs using anti-corrosive agents (p. 030001). Retrieved from https://doi.org/10.1063/5.0102996

Martínez-Barrera, G., Gencel, O., Reis, J. M. L. dos, & del Coz Díaz, J. J. (2017). Novel Technologies and Applications for Construction Materials 2016. *Advances in Materials Science and Engineering*, 2017, 1–2. Retrieved from https://doi.org/10.1155/2017/9343051

Nayak, C. B. (2021). Experimental and numerical investigation on compressive and flexural behavior of structural steel tubular beams strengthened with AFRP composites. *Journal of King Saud University - Engineering Sciences*, 33(2), 88–94. Retrieved from https://doi.org/10.1016/j.jksues.2020.02.001

Peschard, A., Govin, A., Grosseau, P., Guilhot, B., & Guyonnet, R. (2004). Effect of polysaccharides on the hydration of cement paste at early ages. *Cement and Concrete Research*, 34(11), 2153–2158. Retrieved from https://doi.org/10.1016/j.cemconres.2004.04.001

Peschard, A., Govin, A., Pourchez, J., Fredon, E., Bertrand, L., Maximilien, S., & Guilhot, B. (2006). Effect of polysaccharides on the hydration of cement suspension. *Journal of the European Ceramic Society*, 26(8), 1439–1445. Retrieved from https://doi.org/10.1016/j.jeurceramsoc.2005.02.005

Poinot, T., Govin, A., & Grosseau, P. (2013). Impact of hydroxypropylguars on the early age hydration of Portland cement. *Cement and Concrete Research*, 44, 69–76. Retrieved from https://doi.org/10.1016/j.cemconres.2012.10.010

Pourchez, J., Govin, A., Grosseau, P., Guyonnet, R., Guilhot, B., & Ruot, B. (2006). Alkaline stability of cellulose ethers and impact of their degradation products on cement hydration. *Cement and Concrete Research*, 36(7), 1252–1256. Retrieved from https://doi.org/10.1016/j.cemconres.2006.03.028

Saafi, M., & Toutanji, H. (1998). Flexural capacity of prestressed concrete beams reinforced with aramid fiber reinforced polymer (AFRP) rectangular tendons. *Construction and Building Materials*, 12(5), 245–249. Retrieved from https://doi.org/10.1016/S0950-0618(98)00016-6

Sarfarazi, V., Ghazvinian, A., Schubert, W., Nejati, H. R., & Hadei, R. (2016). A New Approach for Measurement of Tensile Strength of Concrete. *Periodica Polytechnica Civil Engineering*, 60(2), 199–203. Retrieved from https://doi.org/10.3311/PPci.8328

Shanmugasundaram, S., Mohanraj, R., Senthilkumar, S., & Padmapoorani, P. (2022). Torsional performance of reinforced concrete beam with carbon fiber and aramid fiber laminates. *Revista de La Construcción*, 21(2), 329–337. Retrieved from https://doi.org/10.7764/RDLC.21.2.329

Shen, D., Wang, X., Cheng, D., Zhang, J., & Jiang, G. (2016). Effect of internal curing with super absorbent polymers on autogenous shrinkage of concrete at early age. *Construction and Building Materials*, 106, 512–522. Retrieved from https://doi.org/10.1016/j.conbuildmat.2015.12.115

Susilorini, Rr. M. I. R., Hardjasaputra, H., Tudjono, S., Hapsari, G., Wahyu, S. R., Hadikusumo, G., & Sucipto, J. (2014). The Advantage of Natural Polymer Modified Mortar with Seaweed: Green Construction Material Innovation for Sustainable Concrete. *Procedia Engineering*, 95, 419–425. Retrieved from https://doi.org/10.1016/j.proeng.2014.12.201

Togerö, Å. (2006). Leaching of Hazardous Substances from Additives and Admixtures in Concrete. *Environmental Engineering Science*, 23(1), 102–117. Retrieved from https://doi.org/10.1089/ees.2006.23.102

Toutanji, H., & Deng, Y. (2002). Strength and durability performance of concrete axially loaded members confined with AFRP composite sheets. *Composites Part B: Engineering*, 33(4), 255–261. Retrieved from https://doi.org/10.1016/S1359-8368(02)00016-1

Wang, Y., & Wu, H. (2010). Experimental Investigation on Square High-Strength Concrete Short Columns Confined with AFRP Sheets. *Journal of Composites for Construction*, 14(3), 346–351. Retrieved from https://doi.org/10.1061/(ASCE)CC.1943-5614.0000090

Wee, T. H., Suryavanshi, A. K., & Tin, S. S. (1999). Influence of aggregate fraction in the mix on the reliability of the rapid chloride permeability test. *Cement and Concrete Composites*, 21(1), 59–72. Retrieved from https://doi.org/10.1016/S0958-9465(98)00039-0

Wei, Y., Guo, W., & Zheng, X. (2016). Integrated shrinkage, relative humidity, strength development, and cracking potential of internally cured concrete exposed to different drying conditions. *Drying Technology*, 34(7), 741–752. Retrieved from https://doi.org/10.1080/07373937.2015.1072549

Wu, Y.-Y., Que, L., Cui, Z., & Lambert, P. (2019). Physical Properties of Concrete Containing Graphene Oxide Nanosheets. *Materials*, 12(10), 1707. Retrieved from https://doi.org/10.3390/ma12101707

Yahyaei-Moayyed, M., & Taheri, F. (2011). Experimental and computational investigations into creep response of AFRP reinforced timber beams. *Composite Structures*, 93(2), 616–628. Retrieved from https://doi.org/10.1016/j.compstruct.2010.08.017

Yuvaraj, K., & Ramesh, S. (2021). Experimental investigation on strength properties of concrete incorporating ground pond ash. *Cement Wapno Beton*, 26, 253–262.

Zaharuddin, N. D., Noordin, M. I., & Kadivar, A. (2014). The Use of (Okra) Gum in Sustaining the Release of Propranolol Hydrochloride in a Solid Oral Dosage Form. *BioMed Research International*, 2014, 1–8. Retrieved from https://doi.org/10.1155/2014/735891

Zhang, H., Li, H., Corbi, I., Corbi, O., Wu, G., Zhao, C., & Cao, T. (2018). AFRP Influence on Parallel Bamboo Strand Lumber Beams. *Sensors*, 18(9), 2854. Retrieved from https://doi.org/10.3390/s18092854